NATIONAL AERONAUTICS AND SPACE ADMINISTRATION

Technical Report 32-1250

Design, Test, and Performance of the Mariner V Temperature Control Reference

W. F. Carroll

JET PROPULSION LABORATORY
CALIFORNIA INSTITUTE OF TECHNOLOGY
PASADENA, CALIFORNIA

April 1, 1968

NATIONAL AERONAUTICS AND SPACE ADMINISTRATION

Technical Report 32-1250

Design, Test, and Performance of the Mariner V Temperature Control Reference

W. F. Carroll

Approved by:

H E Martens

H. E. Martens, *Manager*
Materials Section

JET PROPULSION LABORATORY
CALIFORNIA INSTITUTE OF TECHNOLOGY
PASADENA, CALIFORNIA

April 1, 1968

Contents

Contents (contd)

Tables

Figures

Abstract

The *Mariner V* Temperature Control Reference (TCR) was designed to measure, in space, the net solar thermal energy absorbed by typical spacecraft temperature control surfaces for correlation with laboratory measurements, solar simulation, and materials environmental testing. Valuable information was obtained during the *Mariner V* mission to Venus in 1967. The white surfaces, S-13 and S-13M, degraded more rapidly than had been predicted from laboratory testing. The black, which was intended to provide a reference to solar simulator intensity, demonstrated an unexpected decrease in the product $S\alpha_s/\epsilon$ of the order of 4%. The design, testing, and performance of the equipment and the indicated data on the coatings are discussed in detail.

Design, Test, and Performance of the *Mariner V* Temperature Control Reference

I. Introduction

The purpose of the *Mariner V* Temperature Control Reference (TCR) was to measure in space the net solar thermal energy absorbed by typical spacecraft temperature control surfaces, for correlation with solar thermal simulation and laboratory measurements of thermal radiative properties. In addition, the change in absorbed energy with time in space could be determined for correlation with laboratory materials testing. Problems in measurements, laboratory testing, and correlation with space have been extensively studied (Ref. 1).

The *Mariner V* TCR consisted of three assemblies, one located at the end of each of three solar panels on the *Mariner V* vehicle (Fig. 1). Each assembly (Fig. 2) was identical except for the coatings used and the optional range selected for the temperature transducer. A TCR was not included on the fourth solar panel because of possible interference with the UHF dual frequency receiver (DFR) antenna.

Mariner V was launched June 14, 1967, and encountered Venus October 19, 1967. The flight resulted in the obtaining of additional information of that planet (especially atmospheric characteristics) and data on interplanetary space. The spacecraft, oriented with the sun, maintained three axis stabilization by locking on the star Canopus. Thus, the TCR assemblies were continuously sunlit, and normal to incident solar radiation to within less than $\pm\frac{1}{2}$ deg. Launch occurred near earth aphelion at 1.02 AU, and encounter with Venus occurred at 0.72 AU. The solar intensity varied as shown in Fig. 3; the accumulated solar irradiation is shown in Fig. 4.

The conceptual design, including configuration, instrumentation, and location was done early in 1966.[1] Many refinements and modifications were made, but the basic design concept remained the same. Each TCR was implemented to measure the resistance of a calibrated platinum element and, thus, the temperature of a flat plate normal to the sun and radiating from both sides. From this temperature and suitable corrections for conduction losses, the product $S\alpha_s/\epsilon$ can be computed.

[1]By D. W. Lewis, Jet Propulsion Laboratory.

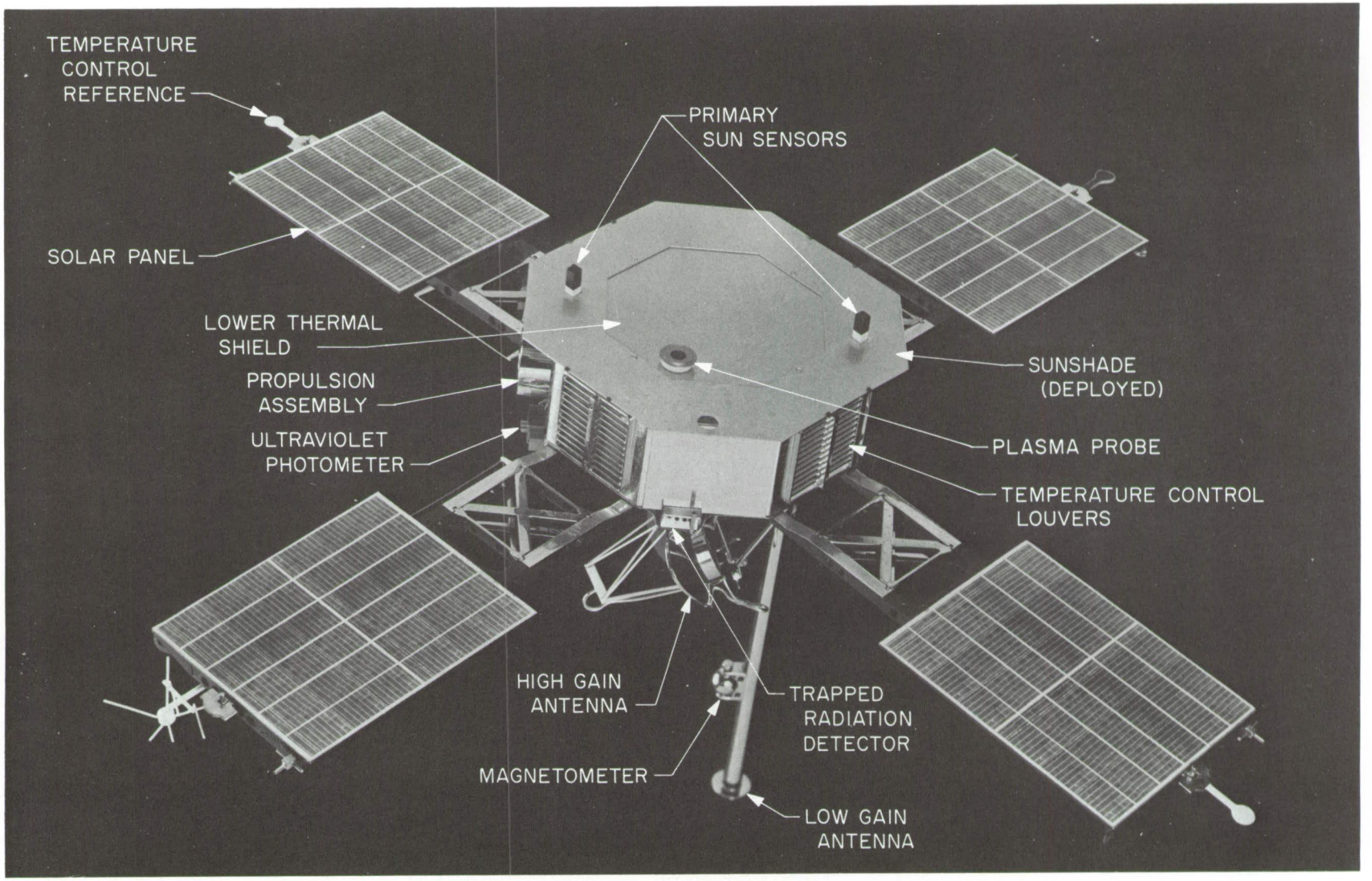

Fig. 1. *Mariner V* spacecraft

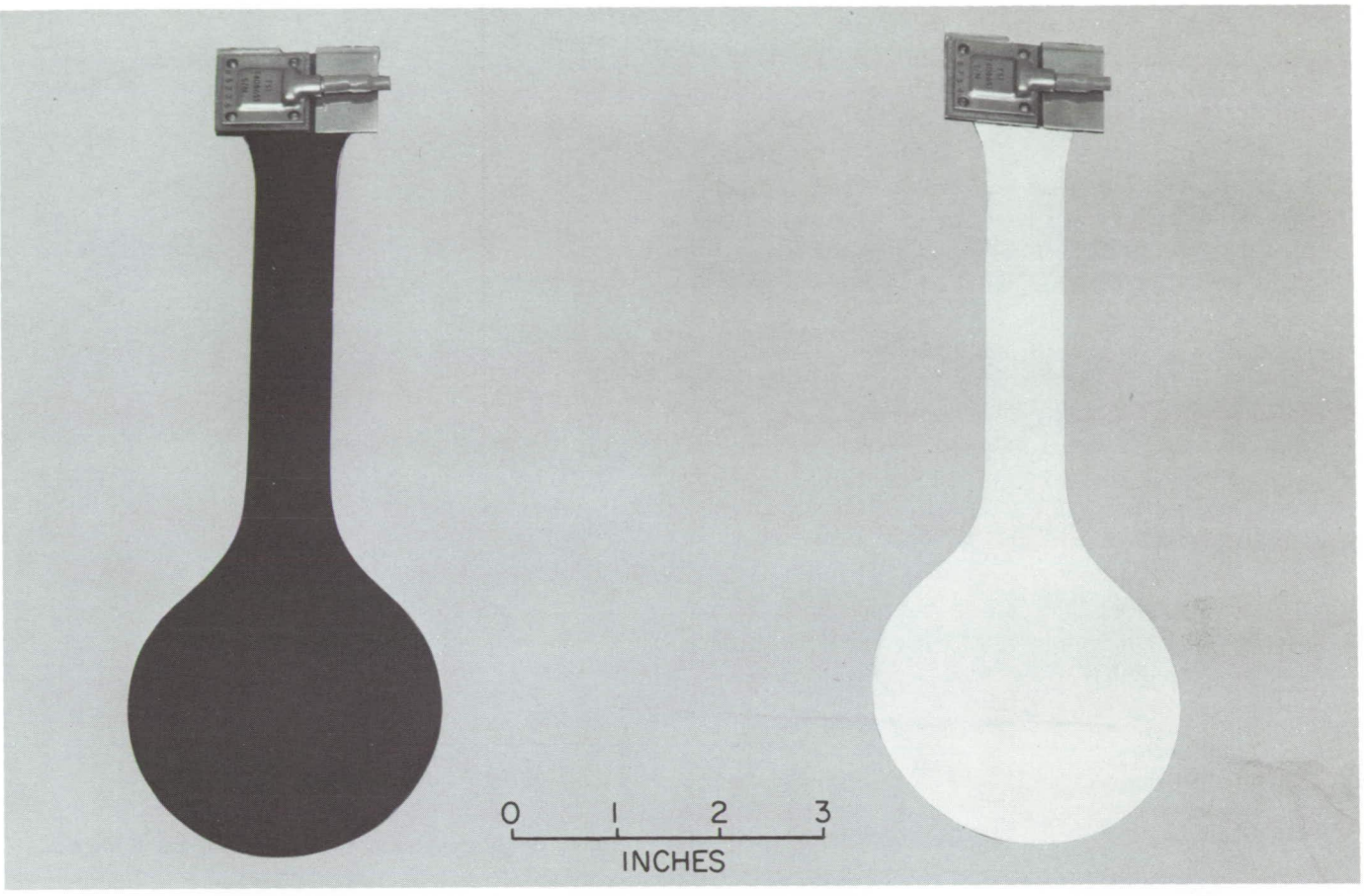

Fig. 2. TCR assemblies

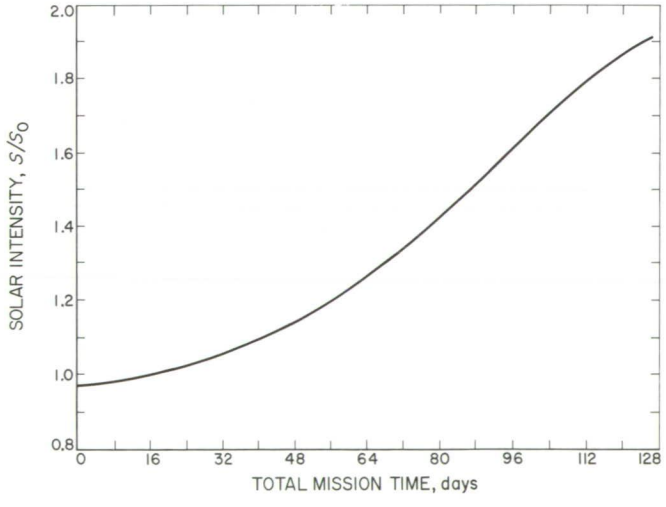

Fig. 3. Solar intensity, *Mariner V* mission

Separation of the terms would be desirable but would require a system of much more complexity than the TCR. The net quantity $S\alpha/\varepsilon$ is of interest for spacecraft temperature control and, particularly in the case of the black, is of significant interest for simulation testing of future space vehicles.

II. Coating Selection

The coatings selected for use on the sunlit surfaces of the TCR assemblies are described in Appendix A. Briefly, they were,

(1) Cat-A-Lac Flat Black.[2] This widely used spacecraft coating was one of the test surfaces on the

[2]Finch Paint and Chemical Company, Torrance. Calif.

Mariner IV Absorptivity Standard (Ref. 2). The reflectance does not vary significantly with wavelength, so it is insensitive to spectral discrepancies between the sun and a solar simulator. *Mariner IV* data indicated stability in the space environment.

(2) S-13 White. This is a widely used spacecraft coating which was known to degrade, but not as much so as the TCR results have shown. This white was used on the TCR because of its general engineering interest and its use elsewhere on the *Mariner V* vehicle.

(3) S-13M White. This is an experimental coating which was undergoing development at the time of the *Mariner V* Project. Laboratory results indicated that it was substantially more stable than S-13; and it was of interest primarily for use on future space vehicles.

For durability in handling, and to simplify analysis of performance in solar simulation, the shaded sides of all assemblies were painted with Cat-A-Lac Flat Black.[2]

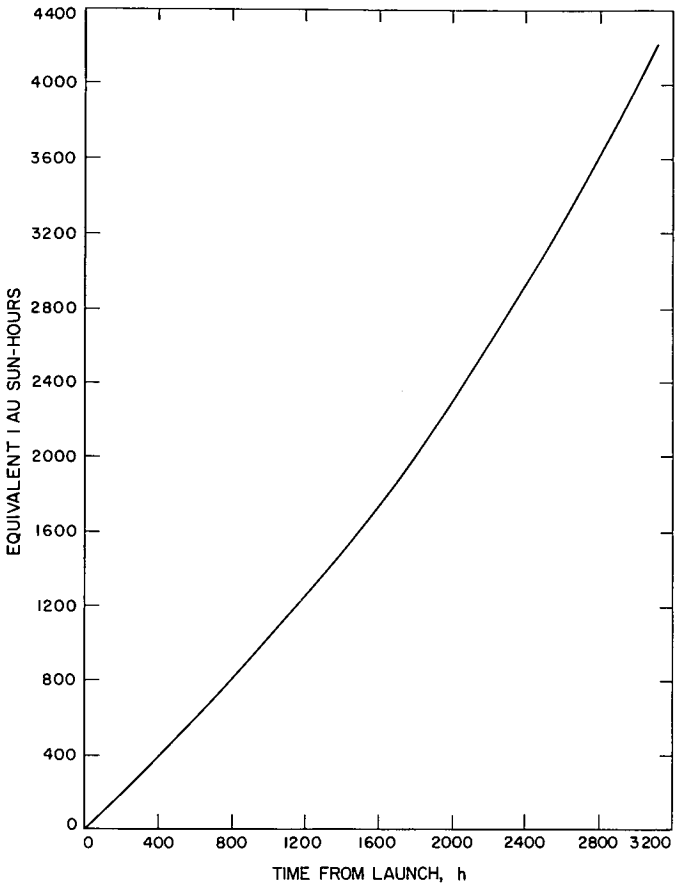

Fig. 4. Equivalent solar exposure, *Mariner V* mission

III. Thermal Design

A. Concept

The thermal balance for the TCR can be idealized[3]:

$$SA_s\alpha_s + \Sigma F_{bus\text{-}TCR}\,\sigma\,(T_{bus}^4 - T_{TCR}^4)\,A_{bus} + \Sigma F_{panel\text{-}TCR}\,\sigma\,(T_{panel}^4 - T_{TCR}^4)\,A_{panel}$$

absorbed solar energy + infrared energy from spacecraft bus components + infrared energy from solar panel and related equipment

$$+ q_{\rho bus} + q_{\rho panel} + \Sigma c_b\,(T_{bracket} - T_{TCR}) + P =$$

+ reflected energy from spacecraft bus which is absorbed + reflected energy from solar panel and related equipment which is absorbed + energy conducted from bracket through leads, support, etc. + internal power

$$\varepsilon_t A_t\,\sigma T_t^4 + \varepsilon_b A_b\,\sigma T_b^4 + \Sigma \varepsilon_a A_a\,\sigma T_a^4 \qquad (1)$$

energy emitted from the isothermal portion of the top surface + energy emitted from the isothermal portion of the bottom surface + energy emitted from all other radiating areas

[3]See *Nomenclature*.

To determine the desired quantity $S\alpha/\varepsilon$ from a flight temperature measurement, the balance of the terms in the equation must be determined or forced by design to be negligible.

The location of the TCR assemblies at the ends of the solar panels reduced radiant coupling with the bus, the second and fourth terms in the above equation, to negligible quantities.

The third and fifth terms were minimized by separating the sensor area from the mounting surface by a web of the maximum length permitted by the dynamic envelope of the launch shroud. Making this web of low conductance material (fiber glass) and coating it the same as the sensor reduced the sixth term to insignificance.

The only internal power dissipation (seventh term in Eq. 1) is that from the 1-mA sampling-current. If this were continuous, it would be less than 0.02% of the incident solar energy. The frequency and duration of sampling further reduced the influence by several orders of magnitude.

Thus, by virtue of the TCR location at the ends of the solar panel, and separation therefrom with a low conductance support, Eq. (1) becomes:

$$SA_s\alpha_s = \varepsilon_t A_t\, \sigma T_t^4 + \varepsilon_b A_b\, \sigma T_b^4 + \Sigma \varepsilon_a A_a\, \sigma T_a^4 \qquad (2)$$

B. Conduction Effects

For small gradients such as those in the TCR, Eq. (2) can be simplified:

$$SA_s\alpha_s = \varepsilon_{average}\,(A_t + A_b)\,\sigma T_{average}^4 + \Sigma \varepsilon_a A_a \sigma T_a^4 \qquad (3)$$

The sensor in the TCR, located near the bottom surface, measured a temperature less than the average, a factor which cannot be neglected. Equation (3) thus becomes

$$SA_s\alpha_s = (\varepsilon_t A_t + \varepsilon_b A_b)\ \sigma\,(T_m + \Delta T)^4 + \Sigma \varepsilon_a A_a \sigma T_a^4 \qquad (4)$$

where

$$\Delta T = f\left(\frac{Qt}{K}\right) \sim f\left(\frac{S\alpha t}{K}\right)$$

where t is the sensor-area thickness and K is the conductance. Thus ΔT is approximately linear with absorbed energy. The value of ΔT was determined analytically and experimentally as described in Appendix B.

The terms in Eq. (4) can be further simplified as a result of TCR design, thermal analysis, and tests. The area containing the sensor was 3 in. in diameter, the center 2 in. of which contained the temperature sensor and a copper mesh to minimize thermal gradients. The ½-in. annulus had low conductance, was coated the same as the sensor area, and thus acts as a *passive guard.*

The thermal balance for the annular area is

$$SA_{as}\alpha_s + C = \Sigma \varepsilon_a A_a \sigma T_a^4$$

and for the 2-in. sensor area,

$$SA_{sen/s}\alpha_s = (\varepsilon_t A_t + \varepsilon_b A_b)\,\sigma\,(T_m + \Delta T)^4 + C \qquad (5)$$

where C is the conductance loss from the sensor to the *guard* area. In Eq. (5)

$$A_{sen/s} = A_t = A_b$$

Thus,

$$S\alpha_s = 2\varepsilon_{average}\,\sigma\,(T_m + \Delta T)^4 + C \qquad (6)$$

The conduction from the sensor to the guard was determined analytically and experimentally as described in Appendix B.

For convenience in data reduction, the correction for the thermal gradient (ΔT) was combined with edge-loss effects to produce a total correction which is a function of measured temperature. For data reduction, Eq. (6) was modified as follows:

$$S\alpha/\varepsilon = 2\,(\sigma T_m^4 + \Delta Q_t + \Delta Q_L) \qquad (7)$$

where

$$\Delta Q_t = \sigma T_{average}^4 - \sigma T_m^4 = \sigma\,(T_m + \Delta T)^4 - \sigma T_m^4$$

and

$$\Delta Q_L = \sigma T_{ideal}^4 - \sigma T_{real}^4$$

While the edge-loss and through-conduction effects are based on nominal values and are treated as additive and independent variables, they tend to be mutually compensating. Higher-than-nominal conductance increases the edge-loss but decreases the effect of through-conductance and vice versa.

Conduction losses through the sensor leads and the supporting web were also determined experimentally and analytically and shown to be insignificant (Appendix B).

C. Temperature Sensor Concept and Design

The TCR was designed to be compatible with the standard *Mariner V* technique for spacecraft temperature measurement on the low-low deck of the data encoder. The available standard-measurement channels measured the voltage drop across temperature transducers due to a 1-mA constant current from the data encoder. The detectable range of the transducer was from 500 to 600 Ω, digitized into a 7-bit binary word, or 126 data number intervals. Most temperature measurements on the spacecraft used identical platinum-resistance thermometers with appropriate series and parallel scaling resistors in the data encoder to adjust the detectable temperature range as desired. It was decided early in the TCR development to strive for maximum resolution and accuracy. Unlike standard transducers, the resistor range of each sensing element was sized to have a resistance slightly above 500 Ω immediately after launch (with the selected coating). An increase in solar intensity or degradation, or both, would increase resistance to 600 Ω, at which time the sensor would go off-scale. No scaling resistors were used in the data encoder.

It was decided that project requirements for spare, test, and flight hardware could best be met at minimum costs of fabrication and test by making a standardized sensor with optional range selection. The final sensor design is shown schematically in Fig. 5 and pictorially in Fig. 6. With this design, all units could be interchangeable until coated and the leads attached. In the event both the flight and spare units of one designation were damaged an alternate spare could be stripped, recoated, and rewired at the terminals as a replacement.

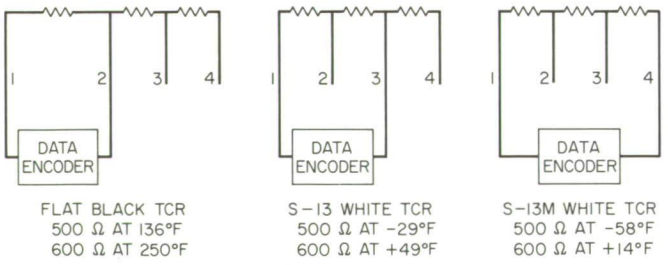

Fig. 5. TCR temperature sensor schematic

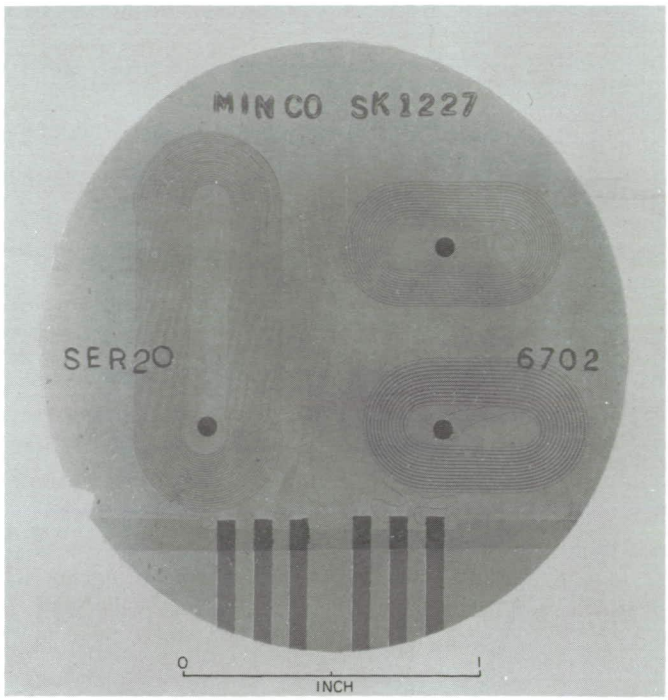

Fig. 6. TCR temperature sensor

Each sensor consisted of three bifilar-wound platinum elements laminated between two layers of Kapton film. The platinum elements were spot-welded to one end of the Alloy 180 terminal strips. During assembly, copper leads encapsulated in the TCR were soldered to these terminals.

D. Sensor Calibration

The sensors were initially calibrated at 0°C by the manufacturer.[4] As part of incoming inspection, the room temperature resistance of each element was checked to verify continuity and resistance value.

After final assembly, the elements in each TCR were calibrated in the Jet Propulsion Laboratory (JPL) Standards Laboratory at −50°, 0°, +50°, +100°, and +120°C. The reported accuracy of initial calibration was ±0.01°C and ±0.005% resistance. After all qualification testing, and before flight, the resistance of each assembly was rechecked at room temperature to assure that no short, drift, or other change had occurred. Two of the assemblies were found to be open (broken spot-welds) following assembly and one sensor was erratic when received from the manufacturer; but there was no change

[4]Minco Products, Inc., Minneapolis, Minn.

in the resistance value of any of the sensors as a result of any testing performed.

When flight data produced an apparent *bleaching* of the black coating, concern arose that the result may have been due to annealing of the sensor element. A prototype (Serial Number 22) which contained an element from the same lot as that used in the black flight unit (Serial Number 19) was subjected to four days at 140°F (the temperature during the early part of the *Mariner V* flight). There was no drift in the sensor resistance. The value at the end of four days, measured at room temperature after the test, agreed with that at the beginning and with the initial calibration approximately nine months earlier.

E. Thermal Tests

A series of tests was performed with TCR assemblies to verify and improve analytical predictions of the TCR thermal performance. These tests are discussed in Appendix B.

IV. Mechanical Configuration

Thermal considerations for mechanical design and location on the spacecraft are discussed in section II.

Mechanical design, development, fabrication, and test are discussed in detail in Appendix C.

V. Flight Results

A. General

Results from the TCR during the early part of the *Mariner V* mission verified equipment design, implementation, and sensitivity. The first data were obtained approximately one-half hour after sun acquisition and all values were within predicted tolerances (including Channel 412, S-13 coated, which was off-scale below −30°F). Subsequent decreases in data number (DN) value of Channels 413 (black) and 432 (S-13M) over the following three hours indicated a decreasing thermal input from the earth early in the mission. A similar effect was noted for the spacecraft solar panels, which could "see" the earth, but not for the lower thermal shield which was turned away from the earth. The resultant lower equilibrium temperatures, apparently beyond earth influence, were still within predicted tolerances.

During the midcourse maneuver all assemblies were cold and off scale, but returned to expected DN values following sun reacquisition. Approximately 1 min after the start of the pitch turn, the black TCR registered a DN of four as compared with pre- and post-midcourse values of five. Approximately 18 min after sun acquisition, both whites registered DN values below pre- and post- values, indicating they had not yet reached thermal equilibrium. The next readings on these channels (40 min later) were 1 DN above pre-midcourse values. From pre-midcourse degradation rates, an increase of 1 DN was expected during the period between the start of midcourse and the first equilibrium data that followed.

The TCR results have raised serious questions about the stability of temperature control coatings in space, and in laboratory testing. The changes in the white TCRs (412 and 432) permit a resolution of changes in solar absorptance to a precision approximately an order of magnitude better than is possible in the laboratory. However, discrepancy between laboratory simulation and testing in actual space amounts to 50% to an order of magnitude disagreement, depending on which laboratory results are used. Deficiencies in laboratory testing, and disagreement among investigators as to anticipated performance in space have long been recognized; but it is clear from the TCR results that very little good simulation testing has been done.

B. White Coatings

At the time of sensor design, good data was not expected very early in the mission; therefore, the temperature range for the S-13 coating was biased upward, to come on scale at a solar absorptance of approximately 0.25 and allow for the initial rapid degradation (as described in Appendix A). The S-13 was expected to degrade and be on scale within 10 to 15 h after launch. Actually, this did not occur until launch + 30 h, indicating either a lower initial solar absorptance or a slower initial degradation rate. From earth input computed from early temperatures for the black and the other white, it can be shown that the absorptance at the first round of data was equal to or less than 0.23.

Early mission data for the S-13M given in Fig. 7 clearly show that degradation started at a consistent rate early in the mission. The initial drop is due to a decrease in earth input. The results are plotted as spacecraft telemetry data number, and the change in relation to

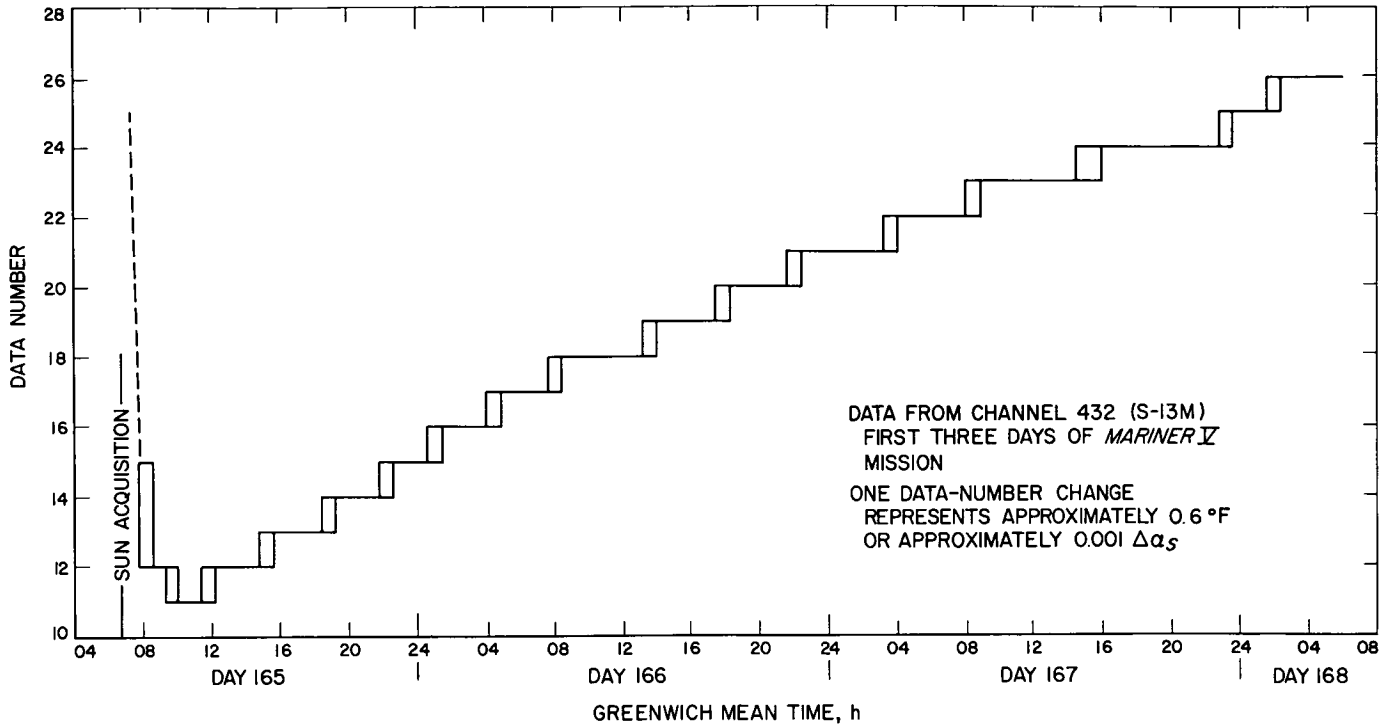

Fig. 7. Early mission data for S-13M white coating

time. No adjustment for change in solar intensity has been made, but this effect is insignificant, less than 0.5%, for the data in Fig. 7. The rectangles indicate the uncertainty associated with data frequency. During this part of the mission a reading was obtained every 42 min. In the range shown, a 1-DN change amounts to approximately 0.001 in the values of α_s. This quantity is less than the valid resolution of measured changes due to laboratory simulation. Thus, by interpolation of flight results, it is possible to resolve degradation rates with an order of magnitude of more precision than is possible in the laboratory. The TCR results will be of great value for correlation with and improvement of laboratory simulation.

Results of degradation of both white coatings are shown in Fig. 8. At the end of these data, the temperature reached the upper limit of the sensor range and no further data were obtained. These curves show apparent solar absorptance vs mission duration, assuming a constant emittance of 0.86 and a solar intensity of 0.878 W/in.^{2} at 1 AU (this value was indicated by early results from the black TCR).

Calculated exposure or "equivalent sun hours" at 1 AU are shown for comparison. At launch, the earth was near aphelion and the intensity was less than that at 1 AU. The spacecraft progressed toward the sun, reaching 1 AU approximately 16 days after launch.

A plot of the ratio α/ε to an initial α/ε would be more valid and eliminate the necessity for assuming values for the emittance and solar intensity and for the assumption that all of the change is in solar absorptance. For comparison, a plot of this kind is shown in Fig. 9. The change in solar absorptance is used primarily to permit a comparison with laboratory data.

For illustration, the same data is plotted as α vs log time in Fig. 10. This form is frequently used for reporting laboratory data and usually shows a straight-line relationship. Caution should be used against overinterpretation of the indicated rates. The indicated rates are of interest in making engineering predictions, and may ultimately be of use for comparing with laboratory simulation. No fundamental significance should be assigned to the shape of the curve, since solar absorptance is an integration of spectral absorptance to an assumed solar energy distribution.

The nature and rate of formation of absorption bands during laboratory simulation may be related to a fundamental energy–material interaction, and similar spectral

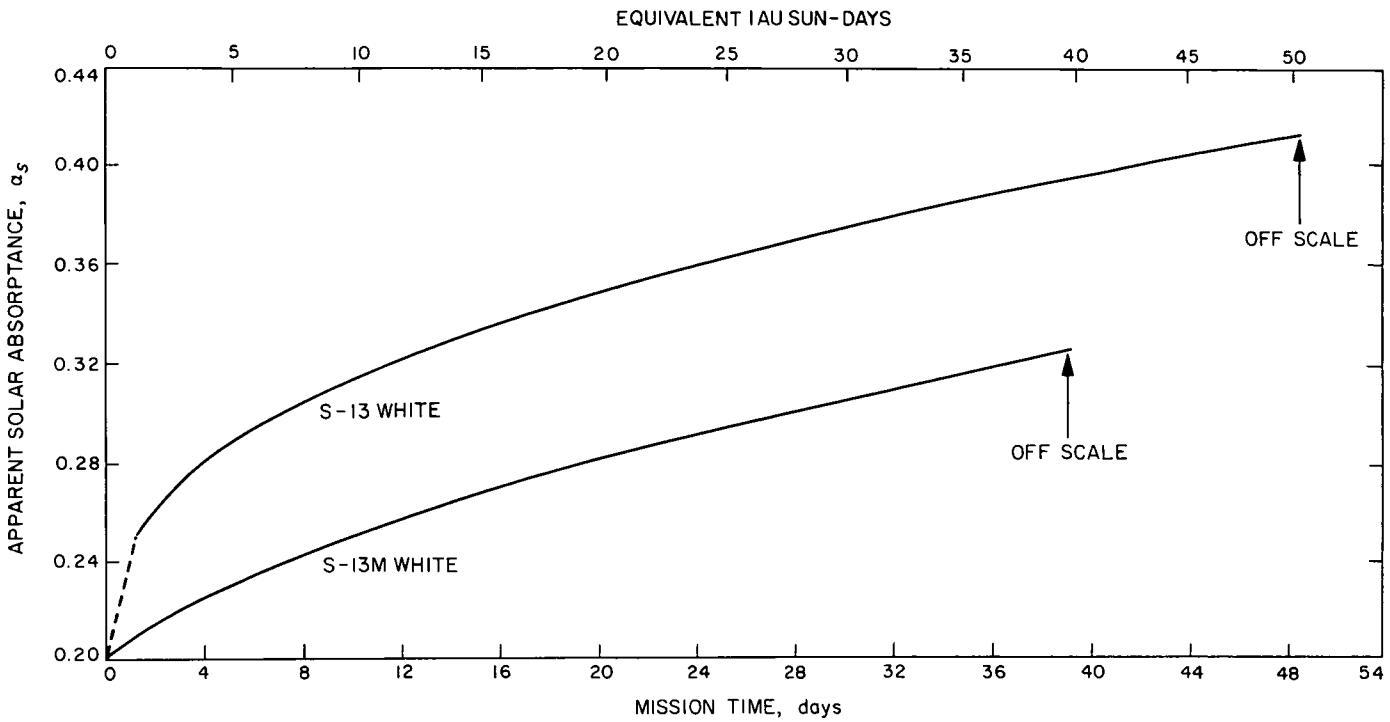

Fig. 8. Solar absorptance of S-13 and S-13M white coatings on *Mariner V* TCR

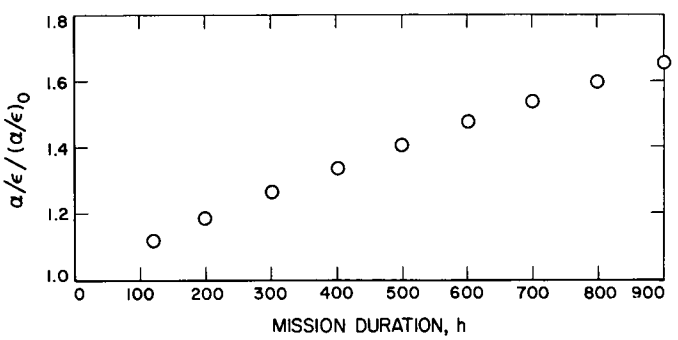

Fig. 9. Degradation of S-13M white coating, shown as α/ε $(\alpha/\varepsilon)_0$

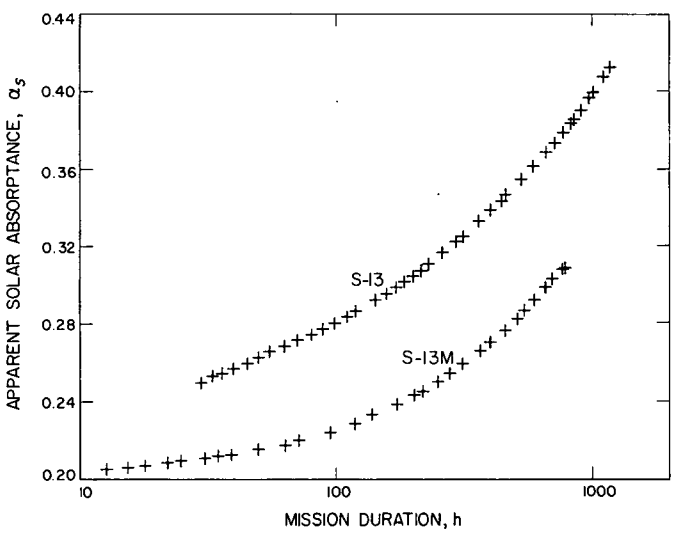

Fig. 10. Degradation of S-13 and S-13M white coatings shown with logarithmic time scale

data from space would be highly useful in analyzing discrepancies between simulation and space. Obtaining such information, however, would require instrumentation and mechanisms much more sophisticated than the TCR.

C. Black Paint

The Cat-A-Lac Flat Black epoxy paint was selected for use on the TCR because it is spectrally insensitive, its properties are well established, and its stability in space was apparently verified by the *Mariner IV* Absorptivity Standard (Ref. 2). It was included primarily to provide a basis for a comparison of absorbed energy in the solar simulator with that experienced in space. The apparent degradation observed was totally unexpected.

Early mission results plotted as the ratio of α/ε to α/ε_0 are shown in Fig. 11. These values are computed at the time switching takes place from one DN to another,

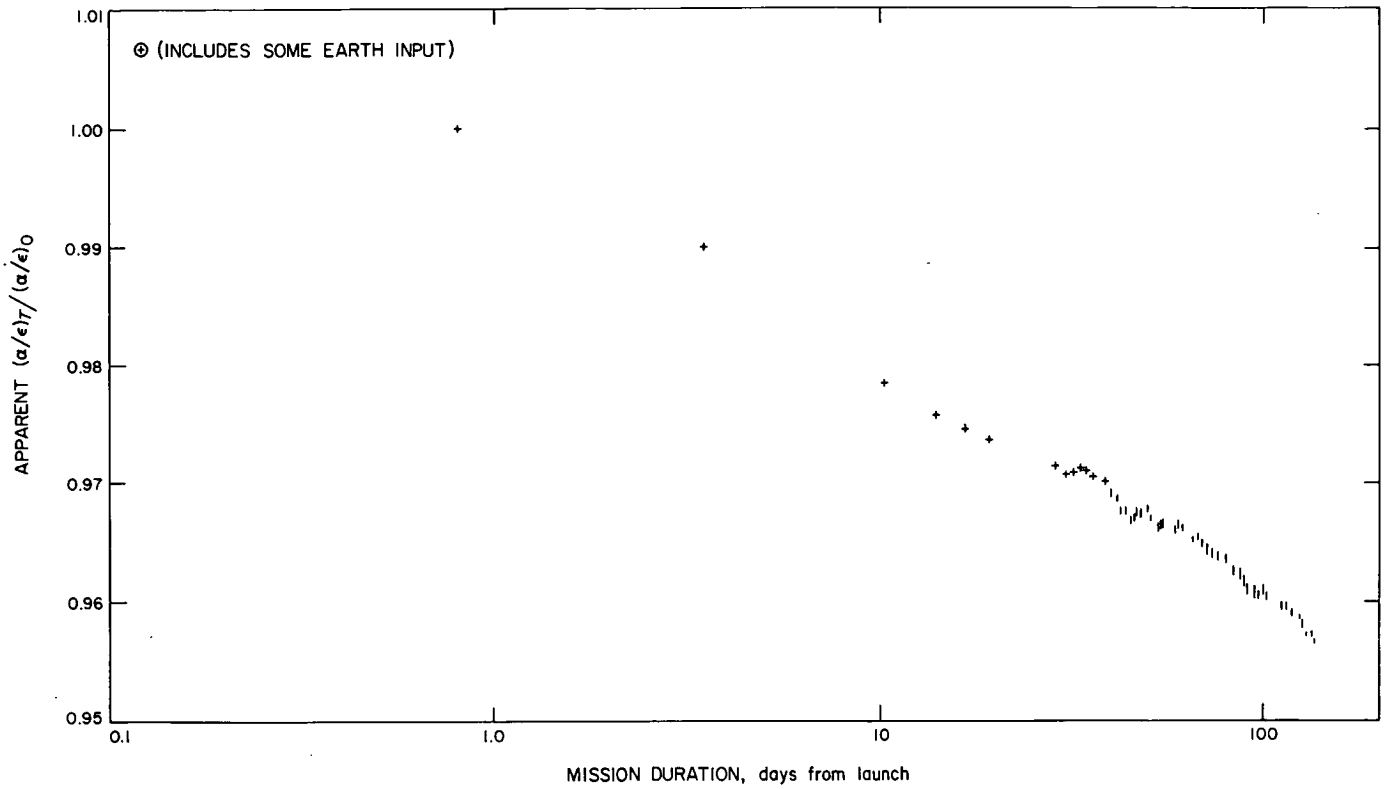

Fig. 11. Black TCR change, apparent α/ϵ with time

assuming that the switch occurs at the midpoint temperature of the nominal calibration values of the data encoder, and that the true temperature is that indicated by calibration data. As long as the temperature interval between switches is the same as the calibration ΔT per DN (0.9°F), and the temperature is within a few degrees of nominal, the precision of the calculation is virtually unaffected by deviations from these assumptions. The first switches showed a decrease in thermal input from the earth, presumably including the switch from 8 to 7 DN, 3 h after launch. The switch from 7 to 6 DN, 20 h after launch, is assumed to represent the initial properties $(\alpha/\epsilon)_0$. The scale shown in Fig. 11 is grossly expanded to show the nature, size, and consistency of the change. This expanded scale is justified by the precision of the instrumentation for at least the first 6 or 8 points, assuming no data encoder shift, since the first 3 switch points are for decreasing temperature and are repeated for the second 3 for increasing temperature. Scale expansion to this size is not justified if it is based on the "accuracy" of the measurements.

The observed bleaching, greater than 4%, was totally unexpected and is significantly larger than anything that has been observed in the laboratory. Simulation testing indicates a change of the order of 1% in solar absorptance for equivalent exposure. This unexplained bleaching, although probably not serious from a thermal control standpoint, further confuses the status of laboratory simulation testing of coatings.

VI. Conclusions and Observations

A. Solar Intensity

Results from the black TCR during the early part of the *Mariner V* mission tend to confirm the recently published value for solar intensity of Stair and Drummond (Refs. 3, 4). This conclusion was reached by assuming nominal instrument and data encoder performance and assuming that the JPL cone radiometer is an absolute device. From these assumptions and results of pre-flight experimental comparison, the solar intensity can be computed. However, the observed degradation, uncertainties in surface properties, uncertainties in conduction effects and, primarily, uncertainties associated with data encoder and spacecraft telemetry make definitive verification impossible. A comparison with the cone radiometer in the JPL 10-ft simulator and the flight results will permit an adjustment of the simulator to a 1-sun level for future testing, independent of the absolute value of solar intensity.

B. Solar Variations

From analysis of time response, sensitivity, and data, it seems reasonable to conclude that there is no variation in thermal energy from the sun, of the order of ½% or greater, for periods of several minutes to a few days. Since a 1-DN change represents approximately a 0.6% difference in absorbed energy, variations considerably less than ½% would be detectable near switch points. No such variations have been seen. Cyclic variations of the order of seconds to several minutes would not be detectable because of the thermal time-constant of the TCR and data sampling rate.

Variations in solar energy over periods greater than several days may not be separable from changes in coating properties or conduction effects. However, additional information may be obtainable from the precise knowledge available of the rate of change of sun–spacecraft distance.

Similarly, there appear to be no significant variations in the energy content of the ultraviolet region of the spectrum during the period for which data were obtained on the white coatings. Both of the white coatings are pigmented with zinc oxide, which characteristically absorbs nearly all of the incident ultraviolet radiation at wavelengths less than 3850 Å. This region, according to Johnson (Ref. 5), constitutes approximately 8% of the total solar energy. These coatings absorb only slightly over 10% of the remaining energy at wavelengths longer than 3850 Å. A change of 5% in the energy content of the ultraviolet region of the spectrum would change the total intensity by only 0.4%, but would increase the absorbed energy by the white coatings by 2.5% and would thus change the indicated temperature by several data numbers. No such variation was seen. As with total intensity, short term variations in the ultraviolet intensity of the order of seconds or minutes would not be detectable, and long-term gradual changes over a period of the order of a month would not be separable from degradation rate or conduction effects.

C. Surface Properties

Initial values from TCRs 413 (black) and 432 (S-13M white) show reasonable agreement with measured surface properties.

The black TCR was somewhat colder (~3°F) after launch, after apparent earth input had decreased to insignificance, indicating a lower α/ε than measured in the laboratory. However, assuming the cone radiometer to be accurate, a comparison with results in the space simulator indicates that the discrepancy is due to solar intensity rather than surface properties, and tends to confirm the solar intensity reported (Refs. 3, 4) as well as measured surface properties.

Channel 432, S-13M, indicated an initial $\alpha/\varepsilon = 0.23$ ($\alpha = 0.20$, $\varepsilon = 0.86$). Lab measurements are $\alpha = 0.18$, $\varepsilon = 0.86$ or $\alpha/\varepsilon = 0.21$. Thus, flight results show a discrepancy of approximately 10% in α/ε. It is unlikely that all of this can be attributed to ε, thus α_s from flight disagrees with lab by approximately 10% or 0.02. A part or even all of this discrepancy may be the result of differences between the flight surface and control samples coated simultaneously. The remainder is probably due to measurement errors or data integration. Solar absorptance is determined by the integration of spectral absorptance against the Johnson (Ref. 5) distribution; since ZnO is a UV absorber, 2% more energy in the UV than is defined by Johnson would account for the 0.02 "discrepancy".

Since channel 412 (S-13 white) was off scale immediately after launch, no comparison between lab measurements of radiative properties and flight results is possible for the S-13 coating.

Considering uncertainties in measurements, solar intensity and spectral distribution, and telemetry uncertainties, there is reasonable agreement between lab measurements of radiative properties and the results obtained in space.

D. Coating Performance and Testing

The results of the *Mariner V* TCR clearly emphasize the glaring deficiency in laboratory simulation of the space environment as it applies to temperature control coatings. These same results should, if properly used, provide a basis for significant improvements in simulation technology which can be applied for future investigations.

VII. Recommendations

The *Mariner V* vehicle provided an almost ideal set of conditions for a measurement of this type. The instrumentation performed as was expected; the "stability" of the coatings was substantially less than anticipated from laboratory simulation. In view of the coating performance results, it would have been advantageous to have increased the range and sacrificed resolution for all three

channels. Such a decrease in resolution would have yielded data on the white coatings over a longer period of time, perhaps indicating some equilibrium condition of degradation.

Incorporation of a precision switching thermometer, such as those used for the *Mariner IV* Absorptivity Standard, in conjunction with a precision resistance thermometer, could have provided a temperature calibration point to eliminate data encoder uncertainties and, in addition, increased the total measurable range.

A significant increase in accuracy could have been achieved for the TCR by reducing the assembly thickness, by increasing the through thermal conductance, or by measuring the true average temperature. These refinements were not possible under the schedule and cost limitations imposed for the *Mariner V* Project.

The poor correlation between laboratory testing and actual space performance indicates the need for improved simulation testing as well as for additional flight experiments of this type.

Experiments to permit separate measurement of S, α_s and ε would be desirable for spacecraft temperature control and would provide a correlation for improved laboratory measurement of radiative properties (α_s and ε).

Appendix A

Coatings Used on the *Mariner V* TCR

I. Cat-A-Lac Flat Black Epoxy

This coating[5] has been extensively used on JPL spacecraft, including *Ranger*, and *Mariners II, IV*, and *V*. It was one of the test surfaces on the *Mariner IV* Absorptivity Standard. The initial *Mariner IV* data (Ref. 2) indicated stability in the space environment, but data obtained from *Mariner IV* during the summer of 1967 (after *Mariner V* launch) permits better resolution of performance and shows evidence of degradation.

This black has an average, nearly uniform reflectance of 4% to 5% throughout the spectral region of significant solar energy. Thus, it is insensitive to spectral distribution and absorbs the same amount of energy (95% to 96%) from the sun as from a solar simulator.

The near normal spectral infrared reflectance from 2μ to 26μ varies between 4% and 22%. The weighted average for near room temperature emittance is 9%. Thus, the calculated near normal emittance (ε_N) = 0.91 and hemispherical emittance (ε_H) = 0.86. This value has an uncertainty of approximately ± 0.04.

The black was used on one TCR assembly primarily to provide a comparison between absorbed energy during solar thermal simulation and in space. Such information would aid in interpretation of differences (if any) between test and flight temperatures. In addition, intensity can be adjusted during testing of future spacecraft to match absorbed energy in space, independent of uncertainties in solar intensity and surface properties (α and ε).

The observed degradation was unexpected and was much greater than the approximately 1% observed during laboratory testing.

II. S-13 White

The S-13 coating, a zinc-oxide-pigmented methyl silicone[6], was developed by IIT Research Institute[7] under JPL contract. It had been used on *Pegasus, Lunar Orbiter,* and several Air Force satellites. It had been selected for use on the *Mariner V* solar plasma and DFR antennas, even though it was known to degrade (the degradation was not detrimental to performance).

Thermal data from the *Pegasus* Micro-Meteoroid satellite indicated serious degradation of the S-13 coating. Subsequent pioneering work, measuring reflectance changes in vacuum during testing by the Lockheed Missiles and Space Company (Ref. 6) confirmed a previously undetected degradation in the near infrared range from about 0.75μ to beyond 2.5μ. The damage, probably associated with desorption of oxygen from the pigment surface, occurs rapidly with irradiation and anneals almost instantaneously upon readmission of air. The occurrence outside the visible region prevented visual detection, and the rapid annealing prevented instrumental detection until capability was developed to make measurements under vacuum. As a result of the Lockheed findings, the entire technology of coatings testing has been changed.

Typically, this infrared damage occurs within a few hours, rapidly reaching an equilibrium change in absorptance of approximately 0.05. Since good TCR data was not expected with the first few hours of the *Mariner V* flight, the sensor range for the S-13 coated assembly was biased upward to come on scale at $\alpha = 0.25$.

III. S-13M White

The S-13M was an experimental white coating under development at the time of the *Mariner V* project. Laboratory results indicated significantly greater stability than the S-13, and it was of interest primarily for use on future space vehicles. S-13M (one of the S-13G series) consists of a silicate-treated zinc oxide pigment in a methyl silicone vehicle. Thus, it is the same as S-13 except for the surface treatment of the pigment.

It had been established by a flight experiment on Orbital Solar Observatory (Ref. 7) and verified in the laboratory that a coating composed of zinc oxide pigment in a potassium silicate vehicle (designated Z-93)

[5]Finch Paint and Chemical Company, Torrance, Calif.

[6]RTV 602. General Electric Company, Downey, Calif.

[7]IIT Research Institute, Chicago, Ill.

did not exhibit the infrared damage described in section II. However, the Z-93 is inorganic and thus is porous, brittle, and difficult to use.

Tests showed that the silicone vehicle was not responsible for the infrared damage. This, plus the preceding evidence, indicated that a silicate treatment of the pigment might preclude the infrared damage and permit formulation of a silicone coating (with less physical property disadvantages than the Z-93) which would not exhibit the infrared damage.

The initial formulation, designated S-13G (subsequent variations have also carried the same designation, which has led to some confusion), verified the initial apparent stability. The residual alkali from the silicate treatment produced a catalyst reaction with the silicone vehicle, causing gelation of the coating and severely limited shelf life. Subsequent work has produced treatment, washing, and redispersion processes which inhibit the gelation and thus extend the shelf life without sacrificing apparent stability.

At the time the sensors were designed and temperature ranges fixed, it was estimated that it would be possible to achieve a solar absorptance of 0.18 with the S-13G modification. At the time the flight sensors were coated, late in 1966, the best achievable α_s was 0.25. Subsequent development at IIT Research Institute achieved α_s between 0.18 and 0.20, much improved shelf life and good apparent stability. Since this version had a lower initial α_s, assembly temperatures would start nearer the bottom of the range and useful data would be obtained for a longer period. In addition, the improved version would provide engineering information of greater validity and interest to future programs. The flight and spare assemblies were recoated at the Air Force Eastern Test Range (Cape Kennedy) during the second week in May 1967.

Appendix B

Thermal Analysis and Test

I. Edge-Loss Analysis

A 22-node computer analysis (Fig. B-1) to determine thermal gradients and effective edge losses was performed[8] in which the TCR was assumed to be a flat disc with no support; the transverse and lateral thermal conductivities were varied around nominal values; and cases were run covering the range of absorbed solar energy expected for all assemblies.

The ideal, infinite flat plate temperature (T_I) was found by making the emittance of the cylindrical areas of nodes 21 and 22 equal to zero. For this case, the temperatures of all odd-numbered (or all even-numbered) nodes are equal and equal to that which the sensor area node would be if there were no conduction loss. Then, by comparison with temperatures for cases where the edge emittance is real, the conduction coupling can be determined as follows: for no radiation from edge, thus no conduction loss,

$$S\alpha = 2\varepsilon\sigma T_{ideal}^4$$

For the sensor area where edge losses are real,

$$S\alpha = 2\varepsilon\sigma T_{real}^4 + C$$

Then

$$C = 2\varepsilon\sigma \left(T_{ideal}^4 - T_{real}^4\right)$$

[8]By D. C. Miller, Jet Propulsion Laboratory.

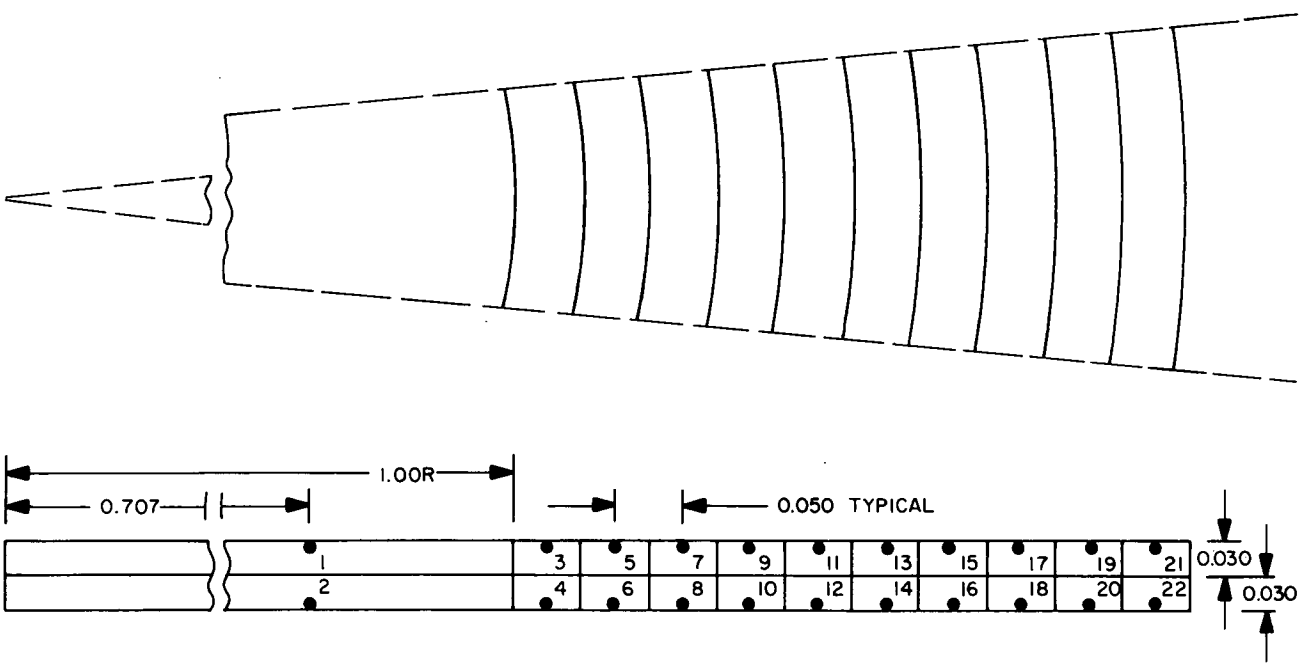

SUNLIT AREAS: NODE 1, CIRCULAR; ODD-NUMBERED NODES 3 THROUGH 21, ANNULAR.
EMITTING AREAS: NODES 2 AND 4, CIRCULAR; NODES 3 THROUGH 22, ANNULAR; IN ADDITION NODES 21 AND 22 HAVE CYLINDRICAL RADIATING AREAS. FOR IDEAL CASE $\epsilon = 0$ FOR THESE CYLINDRICAL AREAS.
NO RADIATION COUPLING BETWEEN NODES.
CONDUCTION COUPLING WITH VARIABLE K BETWEEN ADJACENT NODES.
FOR THIS ANALYSIS, SYSTEM IS AN UNSUPPORTED CYLINDER 3.0 diam x 0.60.

Fig. B-1. Nodes used for edge-loss analysis

For convenience

$$\Delta Q_L = \frac{C}{2\varepsilon} = \sigma T_{ideal}^4 - \sigma T_{real}^4 \text{ (see Eq. 7)}$$

From the results of cases run for various absorbed solar energies ($S\alpha$) and various thermal conductivities, values of ΔQ_L could be computed.

As shown in Fig. B-2, a comparison of the thermal gradient between the sensor (node 1) and a location near the edge (node 17) with experimental results obtained (see section III) indicates that the thermal conductivity is temperature-dependent, not an unreasonable result. The experimental results were used to compute adjusted values of ΔQ_L for the entire anticipated TCR range (see Fig. B-3).

While the magnitude of the edge losses, ΔQ_L, increases with increasing temperature, the effect becomes a smaller percentage of the total energy balance, decreasing from approximately 3% for the white assemblies near earth to approximately 1.6% for the black at Venus. The analysis and experimental results led to the conclusion that the uncertainty in absorbed energy due to uncertainty in edge losses is approximately ±0.2% and is essentially the same over the entire temperature range.

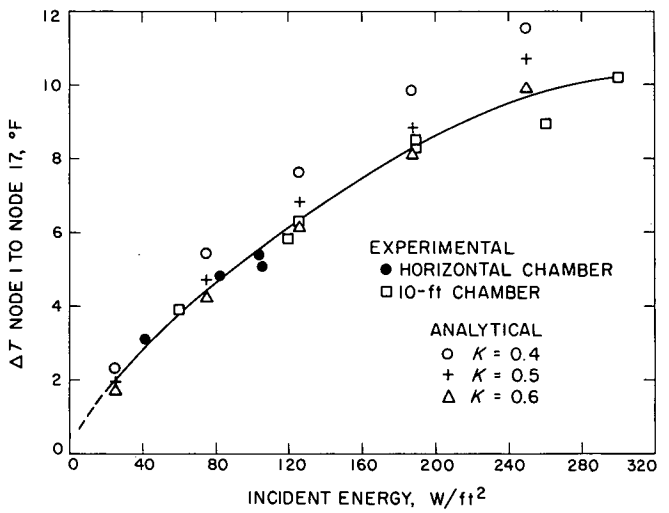

Fig. B-2. Analytical and experimental edge gradient of black TCR

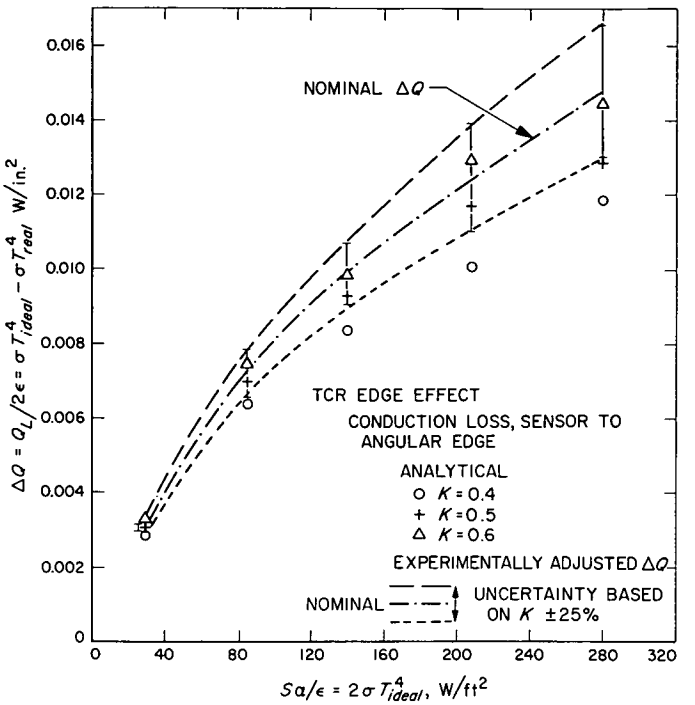

Fig. B-3. Analytically and experimentally adjusted effective edge losses

II. Support Effect Analysis

Preliminary analysis indicated that the influence of the supporting fiber glass T-section, sensor leads, and bracket temperature was small. Subsequently, a 44-node analysis was performed[8] to evaluate these effects in more detail.

Results of this analysis and the experimental results to be discussed, confirm that these effects are insignificant.

III. Gradient and Edge-Loss Tests

A thermal prototype assembly (SN22) was fabricated to verify and refine the thermal analysis of edge-loss effects. In addition to the platinum resistance element, 40-gage copper-constantan thermocouples were imbedded at locations corresponding to nodes 1 and 17 used in the analysis. The thermocouple leads were routed along what should be isothermal lines to minimize lead conduction losses. This assembly was tested in the JPL 10-ft space simulator during the radiometer comparison test as well as the 2 × 4-ft horizontal chamber tests.

Thermal gradients from the sensor area to the edge were measured at five different intensities from 60 to 300 W/ft² during the 10-ft simulator test. Additional data at lower intensities was obtained during the 2 × 4-ft horizontal chamber tests. These results and the adjusted analytical results, already discussed, are shown in Fig. B-3.

For tests in the 2 × 4-ft horizontal chamber, provision was made to rotate the TCR assemblies and permit illumination from either side. The deviation of the sensor temperature from the true average of front and back temperatures was determined by measuring the equilibrium sensor temperature alternately illuminating the assembly from the top and bottom sides. The temperature difference in the two modes of illumination is equal to twice the deviation from true average temperature (Eq. 4). Calculated ideal ΔT, experimental results, and maximum estimated uncertainty values are shown in Fig. B-4.

For convenience in data reduction, values of ΔQ_T were computed over the range of operating temperatures where

$$\Delta Q_T = \sigma T_{average}^4 - \sigma T_M^4 = \sigma (T_M + \Delta T)^4 - \sigma T_M^4$$

(See Eq. 7)

The magnitude of the correction ΔQ_T, and the uncertainty (based on the limits shown in Fig. B-4) in percent of total absorbed energy are approximately 0.6 ±0.3% at −60°F and 1.3 ±0.7% at +40°F (representing the limits of the white samples) and 2.1 ±1.0% at 140°F and 3.4 ±1.7% at 240°F (the limits of the black sample).

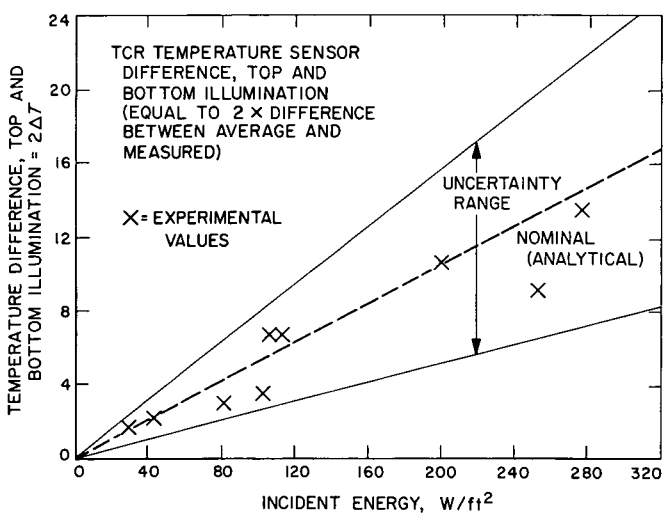

Fig. B-4. Nominal and experimental gradient through TCR

IV. Radiometer Comparison Tests

Three TCR assemblies were included in the radiometer comparison test in the JPL 10-ft space simulator on October 6 and 7, 1966. Those assemblies included in the test were Serial No. 19, which ultimately became the (black coated) flight unit on *Mariner V*, Serial No. 11, which was a type-approval unit, and Serial No. 22, the thermal prototype containing thermocouples.

The tests were run at five different nominal intensities ranging from a nominal of 50 W/ft² to a nominal of 235 W/ft² (actual 60 W/ft² to 300 W/ft²). A comparison of radiometer performance is discussed elsewhere in detail. A comparison of the TCR results with those of the Eppley radiometer and cone radiometer are shown in Table 1. The intensity measured by the cone radiometer is that reported at the time of the test. Since then it has been estimated that these values should be reduced by 3% because of a recalculation of the effective emittance of the cone. The Eppley radiometer Serial No. 5939 was equipped with a 7-degree view limiter and thus detected only direct, simulated, solar radiation. The cone radiometer, with a hemispherical acceptance, "sees" the entire upper hemisphere. The TCR assemblies "see" both the upper and lower hemispheres in the chamber.

An inspection of the results of TCR Serial No. 11 (white) in Table B-1 suggests a grossly decreasing apparent solar absorptance with increasing solar intensity. Since the tests were conducted by starting with the lowest intensity and proceeding to the highest, if any change were to occur the solar absorptance should increase through the test. Thus it is clear that there is a significant reflected solar radiation or infrared input from the chamber during the test.

It can be seen from Table B-1 that excellent agreement existed between Serial Nos. 22 and 19 when adjusted for differences in input intensity in the two locations.

V. Other Thermal Development Tests

A series of tests was conducted in the 2-ft-diameter horizontal chamber using liquid nitrogen cold wall, a quartz window, and the Spectrolab (Model X-25)[9] solar simulator. The test set-up shown in Fig. B-5 was also

[9]Spectrolab, division of Textron, Inc., Sylmar, Calif.

Table B-1. Radiometer comparison test results

Nominal intensity	Measured		Calculated from TCR temperature		Ratios of indicated intensities			Apparent α/ε of white TCR SN 11
	Eppley	Cone	TCR SN22	TCR SN19	I_{22}/I_c	I_{19}/I_c	I_{22}/I_{19}	
50	53	59	62.5	59.4	1.06	1.01	1.05	0.282[b]
100	[a]	121	126.2	120.8	1.04	1.00	1.04	0.263
150	157	191	197.7	187.8	1.04	0.98	1.05	0.257
200	208	263	269.2	256.6	1.02	0.98	1.05	0.256
235	246	312	320.8	300.6	1.03	0.96	1.07	0.251
					1.02[c]	0.98[c]	1.04[c]	

[a]No data available.

[b]Third significant figure valid only for comparison.

[c]Location intensity ratio, based on pre- and post-test intensity measurements.

used for flight acceptance vacuum thermal testing of the flight units.

It was originally intended that these horizontal chamber tests, as well as the flight acceptance tests, provide a "calibration" comparison that could be correlated with the cone radiometer as well as refine the edge-loss effects. These objectives could not be completely met because of nonuniformities in the simulator beam at the test plane. Therefore the best correlation with the cone or other instrumentation can be drawn from the radiometer comparison test.

The effect of conduction along the web of the assembly is discussed elsewhere in this report. The insignificance of this conduction was experimentally verified during this horizontal chamber test. With the 12-in.-diameter simulator beam at 100 W/ft^2 illuminating all except the TCR bracket, the assembly was allowed to come to thermal equilibrium. A mask was then placed in the beam, outside the chamber, shadowing the support web down to approximately three-quarters of an inch from the 3-in. OD of the TCR sensor area. This masking produced a penumbra – a partially shaded area – down to the 3-in. diameter. With this shadowing, the equilibrium sensor temperature was 2.5°F lower than the fully illuminated equilibrium temperature.

An externally controlled heater was installed on the supporting equipment to permit varying the TCR bracket temperature. Raising the temperature of the bracket from −114°F to +150°F produced an 0.1°F increase in the sensor temperature which clearly demonstrated that extreme decoupling had been achieved.

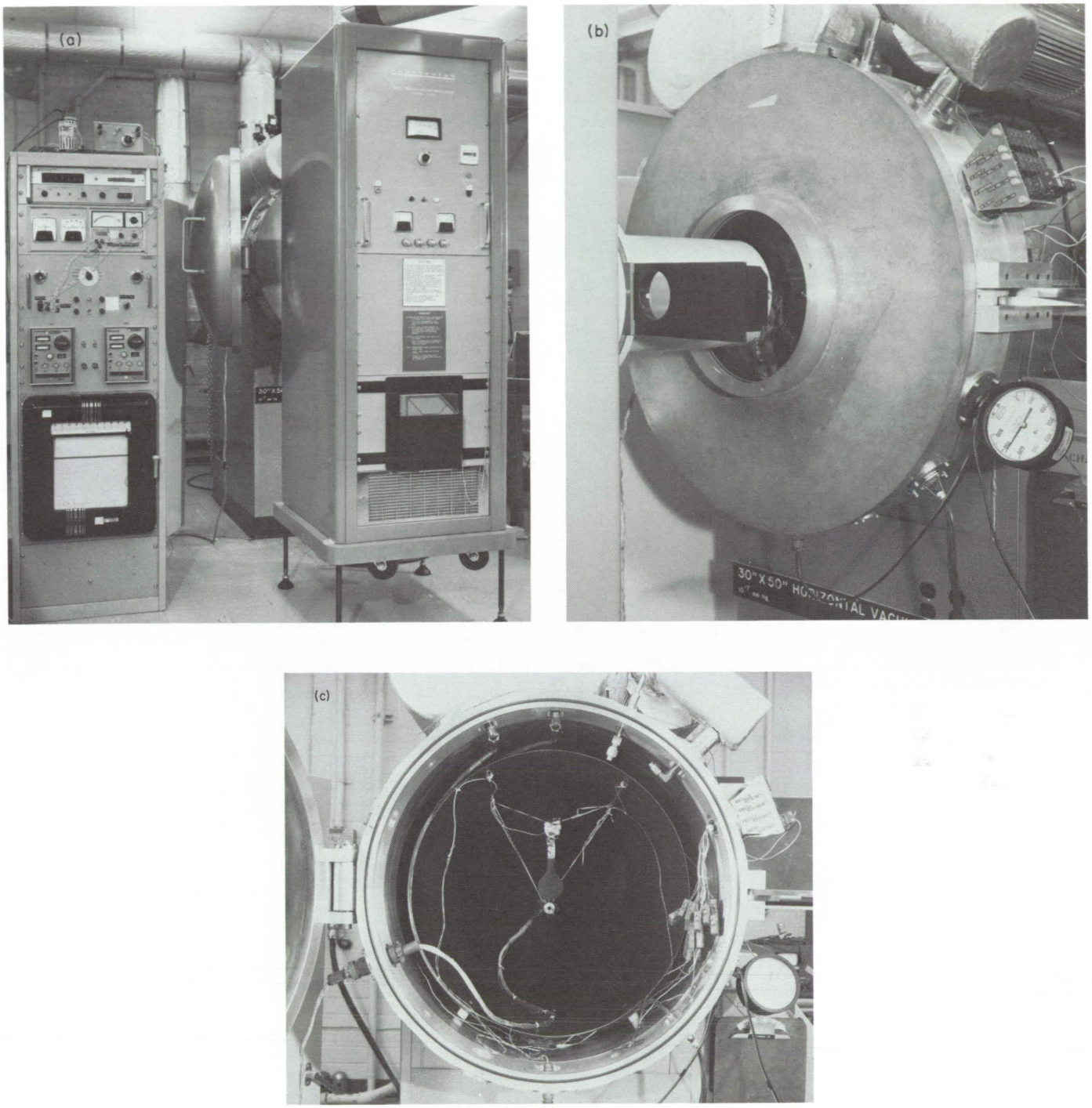

Fig. B-5. TCR thermal test equipment: (a) cone radiometer control and Spectrolab solar simulator; (b) solar simulator installed at quartz chamber window; (c) TCR and cone radiometer test configuration inside cold wall shroud

Appendix C

Mechanical Design and Development

I. Requirements

Thermal considerations of mechanical design and location on the spacecraft are discussed in section III in the text, and Appendix B.

As with most spacecraft hardware, the most severe mechanical requirements on the TCR were those imposed by the launch environment. The size of the sensor, its distance from the end of the solar panel, and its physical excursion during launch were defined by the dynamic envelope of the protective shroud over the spacecraft. In addition, there was a requirement that the resonant frequency (or frequencies) of the TCR assemblies not couple with those of the solar panel because of possible damage to the panels.

II. Prototype Designs

The initial prototypes were fabricated, coated, and readied for tests in two days in order to "piggyback" on a scheduled simulator test. They consisted of a flat sheet of fiber glass, a thermistor, and an aluminum foil disc. As is obvious in hindsight, this configuration proved much too flimsy for suitable suspension in the chamber for testing, although it would have been suitable in gravity-free space. These first prototypes were tested with the *Mariner IV* thermal scale model in the 10-ft JPL simulator, but required suspension at both ends. They were located in the fall-off region of the beam, so the results are subject to question. Because of the errors introduced by suspension and the intensity uncertainty, no serious effort has been made to analyze the experimental data obtained.

A subsequent thermal prototype, mechanically similar to the final flight configuration but containing thermocouples (resistance elements were not yet available), was included in the thermal test of the *Mariner V type approval* solar panel. This prototype included an aluminum foil disc to provide temperature uniformity. Following a thermal shock cycle, the temperature deviated substantially from that which was expected. When the panel was removed for some rework on the panel thermocouples, delamination of the aluminum foil from the TCR assembly was noted. And when the foil was removed, evidence of air pockets could be seen underneath. The foil was replaced with stainless mesh (no copper mesh was available) and the assembly recoated and returned to the test. Performance during a remainder of the solar panel type approval thermal test was nominal, including the survival of a severe, unscheduled thermal shock.

III. Structural Development

While a thin, flat TCR would be thermally ideal and would be suitable once in space, a substantial increase in the rigidity of the support web was necessary for suitable ground testing and for launch vibration. This could be achieved by increasing the thickness of the web or "handle", or by making it a channel, a cylinder, or a T-section. The T-section was recognized as the most difficult to fabricate but was the best for thermal analysis. Furthermore it could most readily be modified to provide the proper resonant frequency or changed as necessary to improve structural stability. A structural analysis provided dimensional requirements for the proper frequencies. But experimental verification was necessary, and it was also necessary to provide for modification should problems arise with resonant frequencies. As has been pointed out, it was necessary that the TCR assemblies not have resonant frequencies which would couple with those of the solar panels.

Two structural development prototypes were fabricated for dynamic testing. One was a lightweight structure made entirely of glass cloth/resin lay-up in the proper configuration. The other was a more conservative conventional design fabricated from prelaminated fiber glass boards and glass/epoxy lay-up.

Each of these prototypes was mounted with its longitudinal axis vertical on a slider plate so that it could be excited laterally by the MBC 70 electromechanical shaker in the critical axis of excitation. A vertical grid was mounted directly behind and a stroboscopic light in front of the prototype. A control accelerometer was mounted to the specimen mounting block. The dynamic response excursions of the assemblies were obtained visually by use of the stroboscopic light and the vertical grid. To determine the resonance band of the assemblies, a run was made at 1 g RMS, 20 to 400 Hz with a

sweep rate of 1 octave per min. (A previous run at 0.25 g RMS over the same range was too low to establish the resonance band.) The structural test consisted of a run made at 12 g RMS starting at 20 Hz, sweeping up to the beginning of the resonance band at 55 Hz, decreasing the gain to 1 g RMS through the resonant band to 75 Hz, then increasing the gain to 12 g RMS and sweeping up to 400 Hz, at a sweep rate of 1 octave per min. After the prototype successfully survived the requisite test levels, the acceleration input in the natural frequency range was increased until failure occurred. Sweeps from 55 to 75 Hz were made at 2 g, 3 g, 4 g, 6 g and 8 g on the heavy structure. A delamination failure occurred at the outboard end of the T-web (where it was expected) at 8 g RMS. The light-weight specimen similarly survived the required test levels and subsequent increase in g level at the resonant frequency to 10 g before failure occurred. It should be noted that these failures were not catastrophic and would not have affected the performance of the TCR or jeopardized the mission had they occurred during a launch.

While the lightweight structure would have been satisfactory, the excursion was somewhat higher and there was a greater possibility of strain or fracture of sensor leads. In addition, more development would have been required for fabrication techniques for the lightweight structure, and scheduled time was severely limited. Therefore, the conservative, somewhat heavier design was selected.

Since no temperature transducers were available, structural mockups were fabricated for use on the Structural Test Model (STM) for initial qualification that were identical to the final flight units except that they did not contain a transducer. Internal encapsulation of the wiring was also the same in order to verify that it would survive vibration. Continuity was checked following the tests and found to be satisfactory.

For the STM tests run later in the program the two type approval units Serial Nos. 11 and 13 were installed in the spacecraft, replacing two of the earlier prototypes.

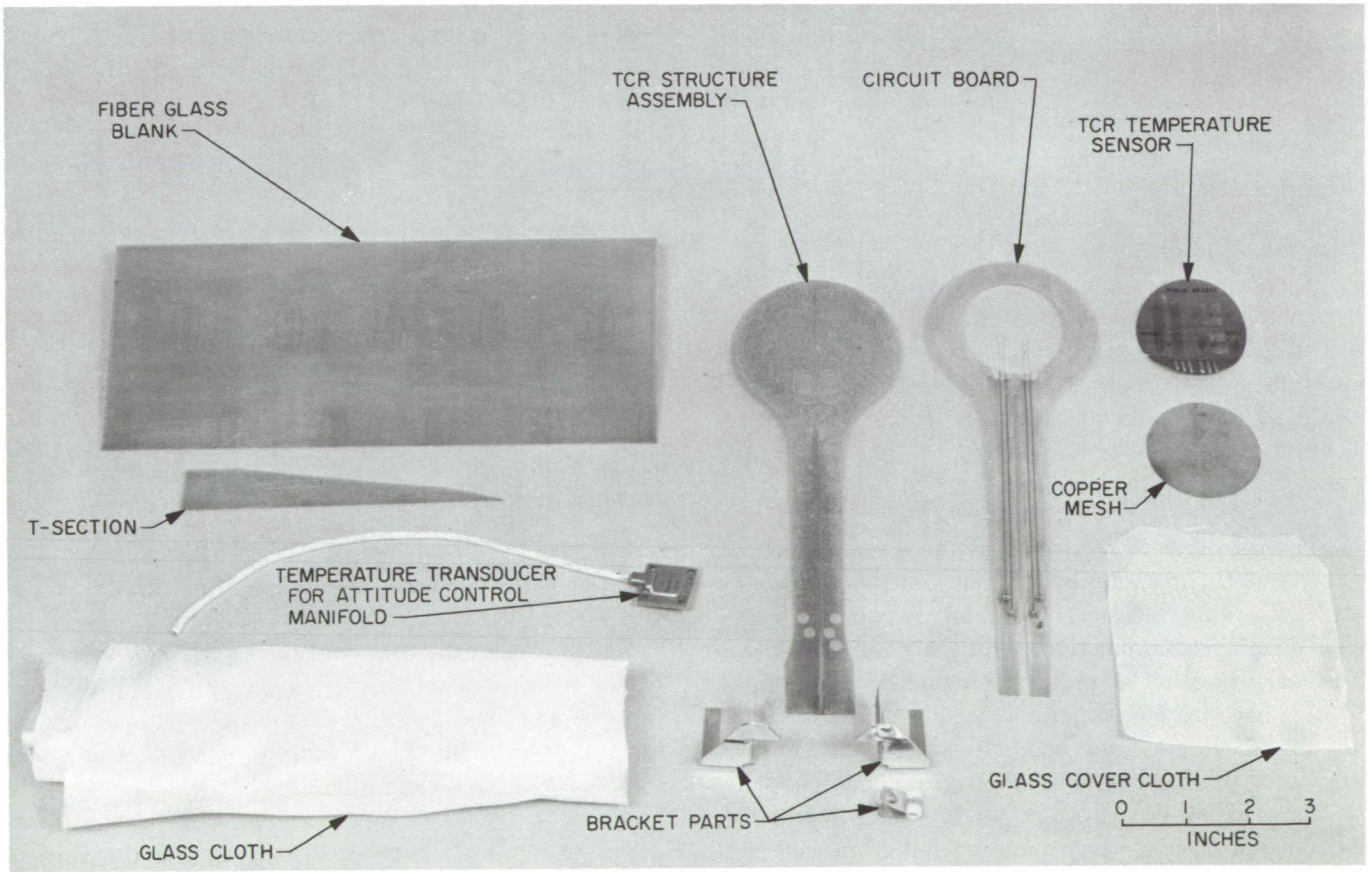

Fig. C-1. TCR components and subassemblies

No problems were detected and no effects of vibration were seen during any of the vibration testing. Significant excursion of the paddles during vibration at their resonant frequency was apparent.

IV. Bracket Design

The TCR bracket attached the fiber glass assembly to the three mounting holes on the attitude control manifold which had been used to attach the solar vanes for *Mariner IV*. In addition, the bracket was required to provide a mounting surface for the temperature transducer used to measure the attitude control manifold temperature. It was desired to bond the bracket to the fiber glass assembly. Satisfactory bonding normally requires a minimum bond thickness and positive pressure on the bond line.

The design of the two-piece bracket assembly shown in Fig. C-1 met all of these requirements and was simple to fabricate. In addition, it will be noted that once the mounting screws and wires were in place, the fiber glass assembly would still be mechanically trapped in the bracket even if the adhesive should fail. Furthermore, the possibility of using mechanical fasteners was not precluded. Likewise, the attitude control manifold temperature transducer, which was bonded in place, could be attached by means of mechanical fasteners should this become necessary. The only complication to this design was the requirement of drilling the mounting holes after assembly because of dimensional variations in the fiber glass assembly and in the bracket parts.

V. Final Mechanical Design and Fabrication

The components which make up the TCR assembly and parts in various stages of fabrication are shown in Fig. C-1. The tapered web for the T-section, cut from a prelaminated epoxy fiber glass board, was attached to a flat board covered with three layers of glass cloth and epoxy resin. This subassembly and later assembly steps (except bracket attachments) were cured in a "vacuum bag". This technique uses a flexible polymer film over the part and with rough evacuation uses atmospheric pressure for uniform pressure over all surfaces. After curing, the flat board was cut to the *lollipop* shape, and requisite areas relieved for soldered joints and terminals.

The circuit board, a 10-mil, prelaminated epoxy fiber glass board, was cut to the shape shown and swaged terminals installed. The board was grooved, relieved as

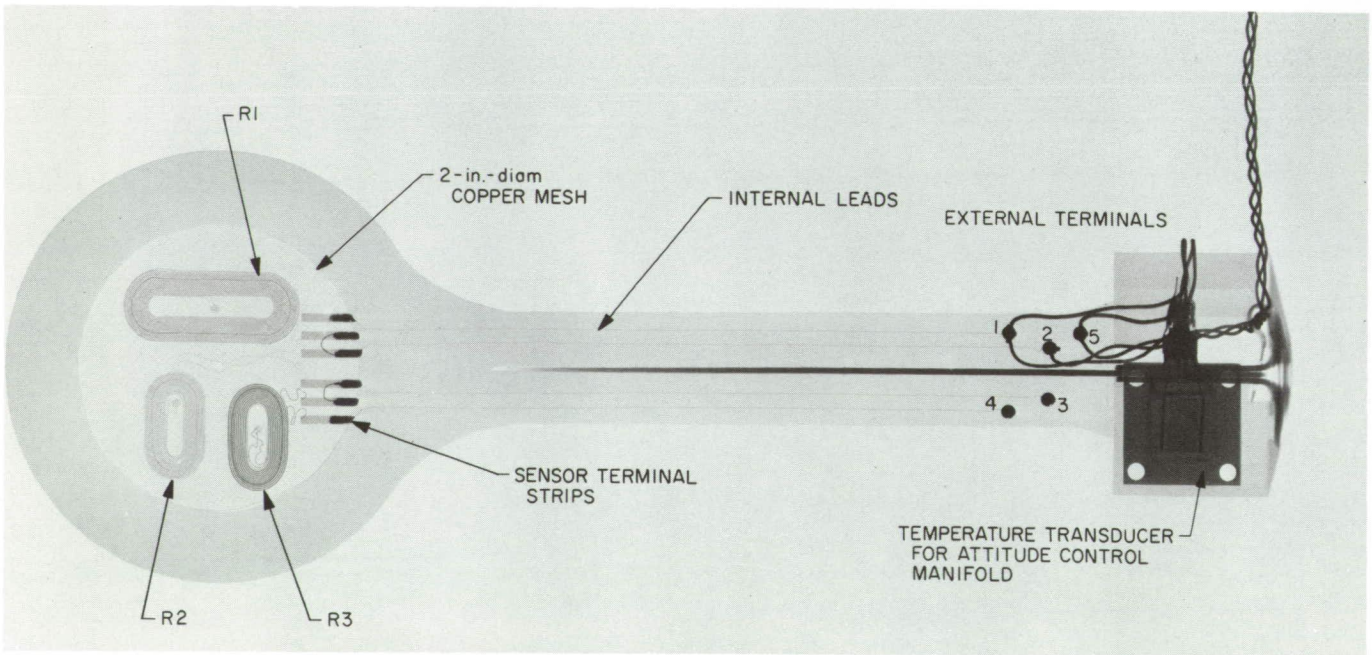

Fig. C-2. Radiograph of assembled TCR

shown, and 6-mil copper wires bonded into the grooves. These wires were soldered into the terminals and to the terminal strips on the temperature sensor to provide positive contact. This terminal board sensor subassembly, the copper screen, and additional layers of glass cloth impregnated with epoxy resin were all bonded in a single operation with a "vacuum-bag" to the structural support subassembly. The copper mesh is included to provide temperature uniformity across the sensor area, and the glass cloth to provide a smooth surface for coating and to increase the strength at the toe of the T-section.

Electrical assembly is best illustrated by the radiograph of a completed TCR shown in Fig. C-2. This black-coated assembly used only the large resistance element and terminals 1 and 2. Terminal 5 is simply a convenient splice to connect the transducer on the bracket which is used to measure the attitude control manifold temperature.

Appendix D

Type Approval and Flight Acceptance Tests

Test requirements for spacecraft hardware include a *type approval* sequence of tests at levels in excess of those expected in flight, the purpose of which is to verify component design and assure design margin. The *flight acceptance* tests are established at levels expected in flight and are intended to verify the components, workmanship, materials, etc., of flight hardware.

A. Type Approval

The type approval sequence included vibration, shock, magnetic susceptibility, and vacuum thermal tests. The vibration, shock, and magnetic susceptibility tests were carried out in accordance with project requirements. The vibration response was expected to be significantly different when mounted to the end of the solar panel than could be simulated by rigid mounting for component test. Thus, it was decided to perform vibration testing aboard the completed spacecraft. Type approval vibration was completed during the second vibration test of the STM vehicle.

Type approval thermal testing included thermal cycling and solar simulation. The thermal cycling consisted of $-220°$ to $+250°$F and return to $-220°$F repeated for two cycles. The assembly was held at each temperature level for 3 to 5 h. Subsequently, each type approval unit was installed in the liquid nitrogen shrouded vacuum chamber with quartz window and illuminated with the Spectrolab solar simulator (*see* Fig. B-5) at approximately 250 W/ft^2 for 1 h. The simulator was then shuttered, allowing the TCR assembly to cool by radiation to the LN2 walls. After 1 h, simulated solar intensity was restored at 250 W/ft^2 and held for an additional hour.

In addition to visual inspection for any damage which may have occurred, the platinum sensors were subjected to calibration check several times during the type approval test sequence. No physical damage or change in sensor calibration was detected.

B. Flight Acceptance

Flight acceptance vibration tests were run aboard the flight spacecraft for the reasons just discussed. Significant excursion of the assemblies at resonant frequency was evident but no damage resulted.

It was intended that the flight acceptance vacuum thermal test provide a "calibration" to the cone radiometer, in addition to verifying flight acceptability. But this calibration with the cone radiometer proved to be impossible because of nonuniform intensity characteristics of the simulator beam, uncertainty in spectrum when used with the white coatings, and the infrared and reflected energy background radiation associated with the test set-up. Thus the radiometer comparison test (*see* Appendix A) provided the best correlation to a measured intensity.

Nomenclature

A area

A_s sunlit area

A_ε emitting area

C energy conducted from the sensor area to the annular "guard"

c simplified conduction coupling term

F radiation exchange form factor (subscripts denote elements)

P internal power dissipation

q_ρ simplified expression which denotes reflected energy from some element absorbed by the TCR

S incident thermal energy flux from the sun

S_0 S at 1 AU (astronomical unit) or 149.6×10^6 km from the sun

T absolute temperature (subscripts denote elements)

T_m measured temperature

α_s solar absorptance

ΔQ_L thermal energy correction term, for conduction losses to "guard"

ΔQ_T thermal energy correction term, for difference between measured and average sensor temperature

Σ summation of several terms

ε emittance (subscripts denote emitting elements)

σ Stefan-Boltzmann constant

References

1. "Thermophysics and Temperature Control of Spacecraft and Entry Vehicles," in *AIAA Progress in Astronautics and Aeronautics: Vol. 18.* Edited by G. B. Heller. Academic Press, New York, 1966.

2. Lewis, D. W., and Thostesen, T. O., "Mariner Mars Absorptance Experiment," in *AIAA Progress in Astronautics and Aeronautics: Vol. 18,* pp. 441–457. Edited by G. B. Heller. Academic Press, New York, 1966.

3. Stair, R., Waters, W. R., Ellis, H. T., "The Solar Constant Based on New Spectral Irradiance Data from 3100 to 5300 Å." (To be published.)

4. Drummond, A. J., Hickey, J. R., Scholes, W. J., and Laue, E. G., "Multichannel Radiometer Measurement of Solar Irradiance," *J. Spacecraft Rockets,* Vol. 4, pp. 1200–1206, Sept. 1967.

5. Johnson, F. S., "The Solar Constant," *J. Meteorol.,* Vol. 11, pp. 431–439, 1954.

6. MacMillan, H. F., et al., "Apparatus for Spectral Bidirectional Reflectance Measurements During Ultraviolet Irradiation in Vacuum," in *AIAA Progress in Astronautics and Aeronautics: Vol. 18,* pp. 129–149. Edited by G. B. Heller. Academic Press, New York, 1966.

7. Pearson, B. D., Jr., "Preliminary Results from the Ames Emissivity Experiment on OSO-II," in *AIAA Progress in Astronautics and Aeronautics: Vol. 18,* pp. 459–472. Edited by G. B. Heller. Academic Press, New York, 1966.